JOURNAL OF PROPULSION AND POWER
Vol. 11, No. 2, March–April 1995

Geometry Effects in the Dynamic Response of Cavitating LE-7 Liquid Oxygen Pump

Takashi Shimura*
National Aerospace Laboratory, Kakuda, Miyagi 981-15, Japan

The dynamic response of the cavitating LE-7 liquid oxygen (LOX) pump, which is essential for POGO analysis of the H-II rocket, was determined by generating sinusoidal flow perturbation with a slit-type perturbation valve installed in the main pump discharge line. In a study of suppressing the LE-7 LOX turbopump rotor vibration due to cavitation, it was found that a kind of rotor vibration, thought to be caused by rotating cavitation, disappeared when a certain geometry of inducer housing was used. Therefore, the effects of inducer-housing geometry on cavitation compliance and on the mass flow gain factor were investigated. Comparison of the test results showed that cavitation compliance for the geometry in which the rotor vibration due to rotating cavitation disappeared was much larger than that for the geometry in which the rotor vibration existed.

Nomenclature

A_i = inducer inlet area, m^2
C_b = cavitation compliance, $-\partial \bar{V}_c/\partial \bar{h}_1$ m^2
C_b^* = nondimensional cavitation compliance, $C_b/(2g\pi dA_i/nu_t^2)$
d = inducer tip diameter, m
f = frequency, Hz
f_c = resonant frequency, Hz
f^* = nondimensional frequency, $f/(nu_t/2\pi^2 d)$
g = gravitational acceleration, m/s^2
$H(s)$ = Laplace transform of fluctuating pressure
h = pressure head, m
h_v = vapor pressure head, m
j = imaginary index
K = cavitation number, $(h_1 - h_v)/(u_t^2/2g)$
k_I^* = damping rate of disturbance
k_R^* = propagation velocity ratio
L = inertance, s^2/m^2
l = axial distance, m
M_b = mass flow gain factor, $-\partial \bar{V}_c/\partial \bar{q}_1$, s
M_b^* = nondimensional mass flow gain factor, $M_b/(\pi d/nu_t)$
N = rotational speed, rpm
NPSH = net positive suction head, $h_1 + v^2/2g - h_v$, m
n = number of inducer blades
Q_m = flow rate per minute, m^3/min
$Q(s)$ = Laplace transform of fluctuating flow
q = flow rate, m^3/s
R = resistance, s/m^2
SS = suction specific speed, $N\sqrt{Q_m}$/NPSH$^{0.75}$
s = complex variable
u_t = tip speed, m/s
V_c = cavity volume, m^3
v = pump inlet flow speed, m/s
Z_c = characteristic impedance, s/m^2
α = phase delay, deg
γ = propagation constant, m^{-1}
ψ = head coefficient, head/(u_t^2/g)
$1 + \mu$ = pump dynamic gain, $1 + \partial(\bar{h}_2 - \bar{h}_1)/\partial \bar{h}_1$

Subscripts
d = downstream
p = pump
u = upstream
0 = large accumulator
1 = pump inlet
2 = pump outlet

Superscripts
~ = fluctuating value
- = mean value

Introduction

POGO is the self-excited longitudinal vibration of rockets due to coupling of rocket structures and propulsion systems, which often occurs in large liquid rockets.[1] In POGO analysis, an accurate description of the characteristics of each component is crucial in order to obtain correct results. With propulsion systems it is well known that the dynamic response of liquid oxygen (LOX) pumps under cavitating conditions is very influential in POGO phenomena. Therefore, accurate dynamic-response data for the cavitating LE-7 LOX pump are critical for the POGO analysis of the H-II rocket.[2] Furthermore, cavitation affects not only system vibration such as POGO, but also local vibration such as rotating cavitation in which the cavitation pattern at the inducer inlet rotates with respect to the inducer blades. Rotating cavitation is considered to cause rotor vibration, and this was the case with the LE-7 LOX pump. However, it was possible to suppress the supersynchronous vibration caused by rotating cavitation in the LE-7 LOX pump almost completely by changing the geometry of the inducer housing[3] as shown in Fig. 1. A theory that explains rotating cavitation phenomena was also presented for the first time.[4] This theory showed that k_I^* and k_R^* were largely affected by a combination of cavitation compliance and the mass flow gain factor as shown in Fig. 2, which is based on Fig. 7 of Ref. 4. Cavitation compliance is defined as cavity volume change rate due to pump inlet pressure fluctuation. The mass flow gain factor is defined as cavity volume change rate due to pump inlet flow fluctuation. Case 1 and case 2 test values and a calculated value, which are plotted in Fig. 2, will be discussed in the results and discussion section. Based on rotor vibration test results and the rotating cavitation theory, it was concluded that the effects of the geometry of the inducer housing on cavitation phenomena were great.

In a study of the dynamic response of the LE-5 rocket engine liquid oxygen pump,[5] components of the pump transfer

Presented as Paper 93-2126 at the AIAA/SAE/ASME/ASEE 29th Joint Propulsion Conference and Exhibit, Monterey, CA, June 28–30, 1993; received July 22, 1993; revision received June 28, 1994; accepted for publication July 19, 1994.

*Senior Researcher, Rocket Propulsion Research Division, Kakuda Research Center. Member AIAA.

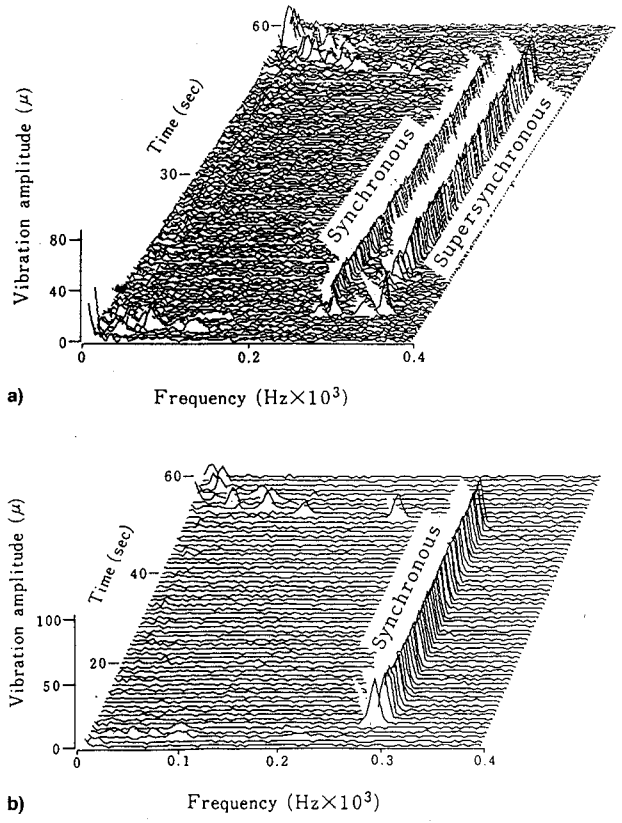

Fig. 1 LE-7 LOX pump rotor vibration: a) original and b) modified inducer housing.

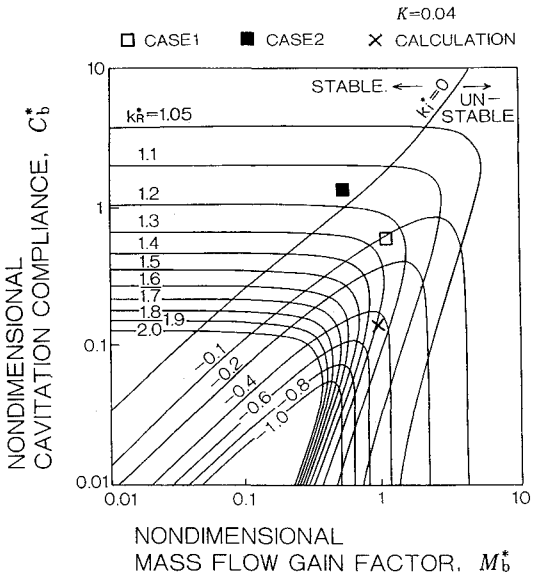

Fig. 2 Effects of M_b^* and K_b^* on rotating cavitation.

matrix,[6] except cavitation compliance and the mass flow gain factor, were determined. It was assumed that cavitation compliance and the mass flow gain factor were estimable by inducer water test results.[7] However, comparison of nondimensional cavitation compliance values between cryogenic fluid test results for rocket pumps and water test results for rocket pump inducers showed that they were considerably different from each other. As to the mass flow gain factor, experimental values for cryogenic fluid tests are few. Consequently, we attempted to determine cavitation compliance and the mass flow gain factor for the cavitating LE-7 LOX pump by generating sinusoidal perturbation in the pump flow. Cavitation compliance and the mass flow gain factor were determined for two geometries of the inducer housing.

One of the most difficult problems in the experiments was measuring the dynamic flow rate of cryogenic fluid. In the present study, a type of rapid-response ultrasonic flow meter[8] was used. This is the only flow meter that can measure the dynamic flow rate of cryogenic fluid without flow disturbance. The flow meter worked well under high-pressure test conditions and made it possible to determine the pump resistance and inertance. Measurement by this flow meter becomes difficult under low-pressure conditions due to diffused reflection from bubbles generated in the line. In the case of the LE-7 LOX pump, because the pump inlet pressure is comparatively high under H-II rocket flight conditions, the flow meter was expected to be usable. However, it was not usable under the estimated pump inlet pressure conditions because of malfunctions caused by ultrasonic signal deterioration due to bubble generation. Therefore, cavitation compliance and the mass flow gain factor could not be determined by use of the dynamic flow rate. Under these circumstances, determination of cavitation compliance and the mass flow gain factor by pressure data was attempted. In this method, the transfer function between the pump outlet fluctuating pressure and the pump inlet fluctuating pressure was determined experimentally by sweep perturbation tests. This transfer function was compared with the transfer function derived from a mathematical model that included pump dynamic response. Substituting cavitation compliance and the mass flow gain factor as parameters into the mathematical transfer function, values which made the mathematical transfer function equal to the experimental transfer function, were determined. These values were assumed to be the true cavitation compliance and the mass flow gain factor.

In the method where cavitation compliance is determined by pressure data, compliance existing in the upstream line of the pump is a big problem. A large accumulator was installed in the vicinity of the pump inlet in order to eliminate the upstream effects. The mass flow gain factor was assumed to exist only in the pump region because it is defined as the cavity volume change rate due to the pump inlet flow rate fluctuation. Thus, by restricting the relatively shorter region of the concerned system extending from the large accumulator to the pump outlet, it was expected to be possible to determine the mass flow gain factor and cavitation compliance by pressure data. However, as a result of installing a large accumulator in the vicinity of the pump inlet, resonant frequency of the pump inlet line increased. Therefore, the effect of the phase delay of the cavity volume change to pressure fluctuation ceased to be negligible. This phase delay considerably reduced the calculated gain of the transfer function between the pump outlet pressure and the pump inlet pressure. Con-

Table 1 Main design values of LE-7 LOX pump

Rotational speed, rpm	20,000
Shaft power, kW	6,400
Main pump flow rate, m³/s	0.2
Main pump pressure rise, MPa	20.9
Main pump impeller tip diameter, mm	196.1
Inducer tip diameter, mm	149.8
Number of inducer blades	3
Inducer tip blade angle, deg	7.5
Inducer inlet flow coefficient	0.0775

Table 2 Dimensions of inducer housing

	Upstream diameter, D_1 mm	Front-half diameter, D_2 mm	Rear-half diameter, D_3 mm
Case 1	150.3	151.0	151.6
Case 2	154.0	151.5	151.5

sequently, the effect of the phase delay was compensated for by use of phase delay values derived from the data in the literature.[7]

Artificial perturbation was generated in the pump discharge line in order to minimize fluctuation in the pump inlet line so that linearity could be maintained. Because we restricted the length of the region of the concerned system extending from the large accumulator to the pump outlet, compressibility of the pipe system was considered to be negligible. However, we attempted to examine the effect of pipe system compressibility by comparing the results for a compressible distributed parameter system model with the results for an incompressible lumped parameter model.

Test Pump

The pump tested was the LE-7 LOX pump, a schematic of which is shown in Fig. 3. Its main design values are given in Table 1, and its performance has been previously reported.[9] Tests were carried out on two geometries, these geometries being shown in Fig. 4. Dimensions of the inducer housing in Fig. 4 are listed in Table 2.

Test Facility and Test Conditions

A schematic of the test facility is shown in Fig. 5. A large accumulator of 0.3-m^3 helium gas capacity was installed in the upstream line, 2.5 m away from the pump. Perturbation was generated by a slit-type perturbation valve installed in the main pump outlet line. The maximum frequency of this perturbation valve is 50 Hz. Dynamic pressure was measured by piezoelectric-type flush-mounted pressure sensors with built-in preamplifiers. Dynamic flow rates were measured by rapid-response ultrasonic flow meters.[8] Initially, pump resistance and inertance values were determined by constant frequency perturbation tests under relatively high pump inlet pressure conditions by the same procedure used for the LE-5 LOX pump.[5] Then, sweep perturbation tests were carried out under

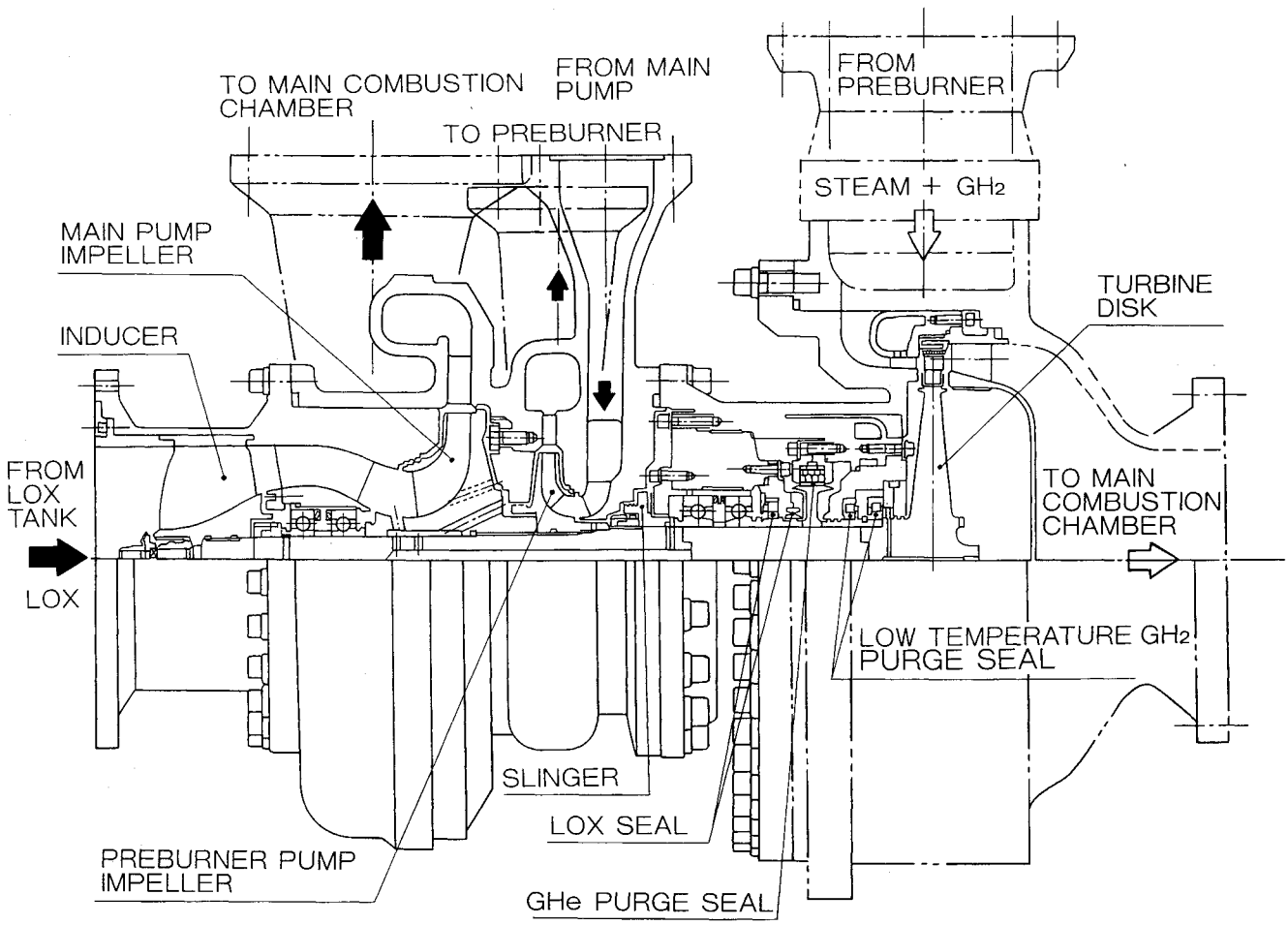

Fig. 3 Schematic of LE-7 LOX pump.

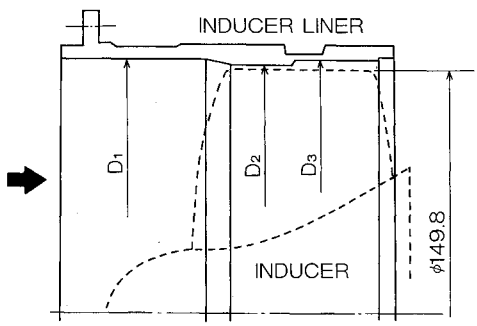

Fig. 4 Geometries of inducer housing.

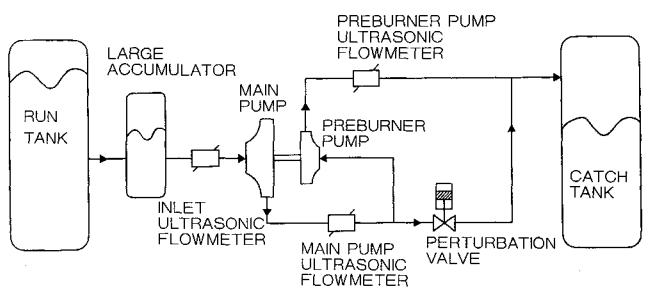

Fig. 5 Schematic diagram of test facility.

Table 3 Pump operating conditions (sweep test)

Test no.	Speed, rpm	Main pump flow rate, %	Cavitation number
	Case 1 geometry		
1	12,500	100	0.056
2	12,500	101	0.052
3	12,500	102	0.041
4	12,500	100	0.030
	Case 2 geometry		
1	9,900	98	0.064
2	9,900	99	0.049
3	12,500	100	0.061
4	12,500	98	0.050
5	12,500	97	0.049
6	12,500	100	0.048
7	12,500	98	0.036
8	12,500	100	0.032
9	15,900	99	0.056
10	16,000	99	0.041

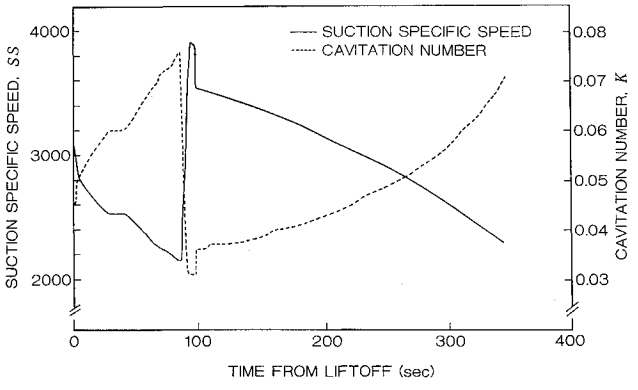

Fig. 6 Predicted suction conditions.

low pump inlet pressure conditions in which dynamic flow rate measurement was impossible. By employing sweep perturbation tests, transfer functions between the pump outlet and inlet pressures were determined. Pump inlet pressure conditions were determined based on predicted conditions during the H-II rocket flight. Figure 6 shows the predicted suction specific speed and cavitation number of the LOX pump during the first-stage flight of the H-II rocket. Around 90 s after liftoff, pump suction conditions become most severe because of the pump inlet pressure decrease due to separation of the solid rocket motors. Besides cavitation number, rotational speed was also selected as a parameter of the sweep perturbation tests. Table 3 shows the pump operational conditions in the sweep perturbation tests. The main pump flow rate is shown as a percent of the flow rate that makes the velocity triangle similar to the design velocity triangle. Liquid nitrogen was used as the pump fluid.

Determination of C_b and M_b

In the present study, a pump dynamic model of lumped parameters was adopted for simplicity, although there is also a nonlumped parameter model.[10] The pump dynamic response was assumed to be shown by C_b, M_b, $1 + \mu$, R_p, and L_p. Phase delay of cavity volume change to pressure fluctuation was included by multiplying C_b by $e^{-j(\alpha\pi/180)}$. Phase delay of cavity volume change to flow fluctuation was neglected because its effect on the transfer function was small. The pump inlet line was assumed to be incompressible and shown by two lumped parameters, namely, R_1 and L_1. Based on these assumptions, the hydraulic system from the large accumulator to the pump outlet was modeled as shown in Fig. 7. Linearized equations of motion and continuity for this model are as follows:

$$-\tilde{h}_1 = R_1\tilde{q}_1 + L_1\frac{d\tilde{q}_1}{dl} \tag{1}$$

$$\tilde{h}_2 - \tilde{h}_1 = \mu\tilde{h}_1 - R_p\tilde{q}_2 - L_p\frac{d\tilde{q}_2}{dt} \tag{2}$$

$$\tilde{q}_2 - \tilde{q}_1 = -C_b e^{-j(\alpha\pi/180)}\frac{d\tilde{h}_1}{dt} - M_b\frac{d\tilde{q}_1}{dt} \tag{3}$$

Based on the pump suction performance test results shown in Fig. 8, $1 + \mu$ was determined to be 1. Suction performance tests under conditions down to breakdown points and perturbation tests under various flow coefficients other than near the design flow coefficient were not carried out due to reasons of safety, and budget and time restrictions on the number of tests that could be conducted. L_p and R_p were determined by constant frequency perturbation tests under high inlet-pressure conditions. R_1, which was very small, was determined by generally used values for pipes. L_1 was determined by constant frequency perturbation tests using the following relation:

$$(\tilde{h}_1/\tilde{q}_1) = -R_1 - j\omega L_1 \tag{4}$$

The L_1 value calculated by pipe geometry was almost the same as the experimental values.

Execution of Laplace transform on Eqs. (1–3) yields:

$$-H_1(s) = R_1Q_1(s) + L_1sQ_2(s) \tag{5}$$

$$H_2(s) - H_1(s) = \mu H_1(s) - R_pQ_2(s) - L_psQ_2(s) \tag{6}$$

$$Q_2(s) - Q_1(s) = -C_b e^{-j(\alpha\pi/180)}sH_1(s) - M_bsQ_1(s) \tag{7}$$

Using Eqs. (5–7), the transfer function between the input $H_2(s)$ and the output $H_1(s)$ was determined as follows:

$$\frac{H_1(s)}{H_2(s)} = \frac{R_1 + L_1s}{\{[1 + \mu + (R_p + L_ps)C_b e^{-j(\alpha\pi/180)}s](R_1 + L_1s) - (R_p + L_ps)(M_bs - 1)\}} \tag{8}$$

Substituting $j2\pi f_c$ into s and other known values except C_b and M_b into the variables, calculation was carried out with C_b and M_b parametrically. Results of the calculation showed that the C_b values that yielded the peak gain of $H_1(s)/H_2(s)$ were scarcely affected by the M_b values. It was also shown that resonant frequency for this C_b was scarcely affected by M_b as shown in Fig. 9. Therefore, this C_b was assumed to be the actual C_b. Substituting this C_b into $H_1(s)/H_2(s)$ and using M_b

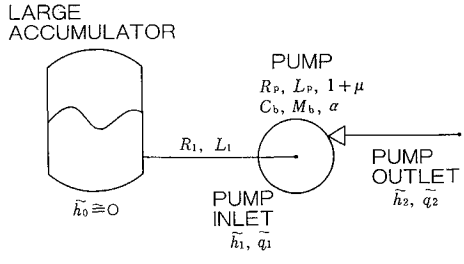

Fig. 7 Model of hydraulic system.

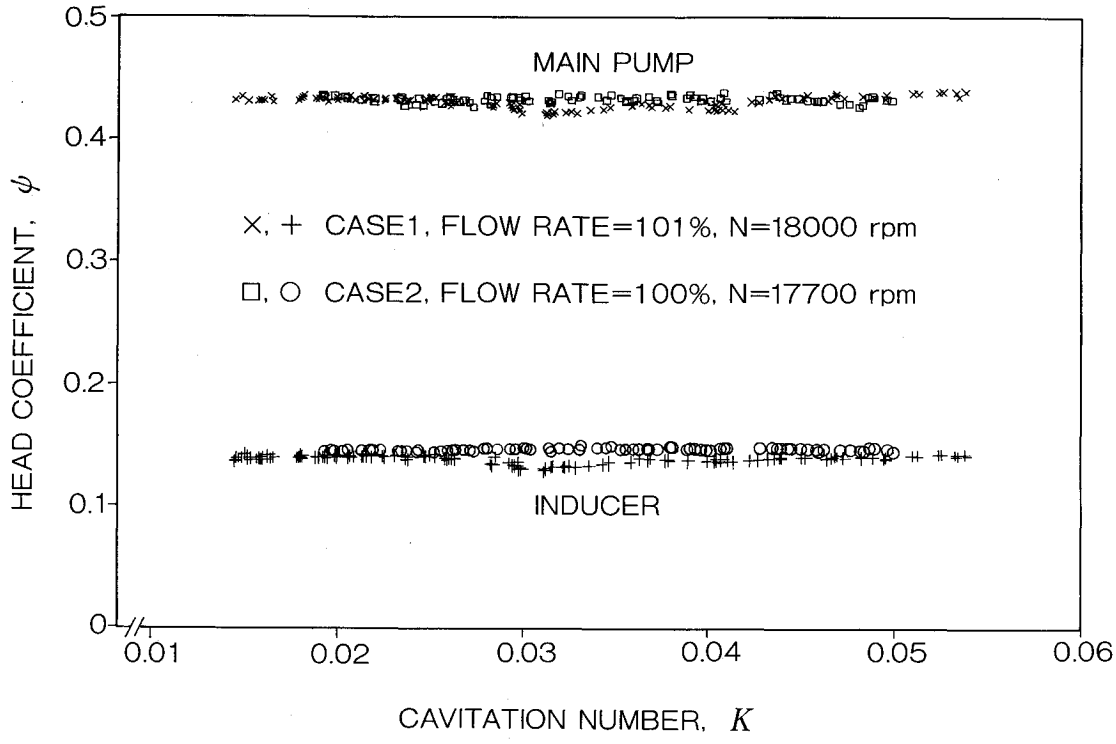

Fig. 8 Suction performance of LE-7 LOX pump.

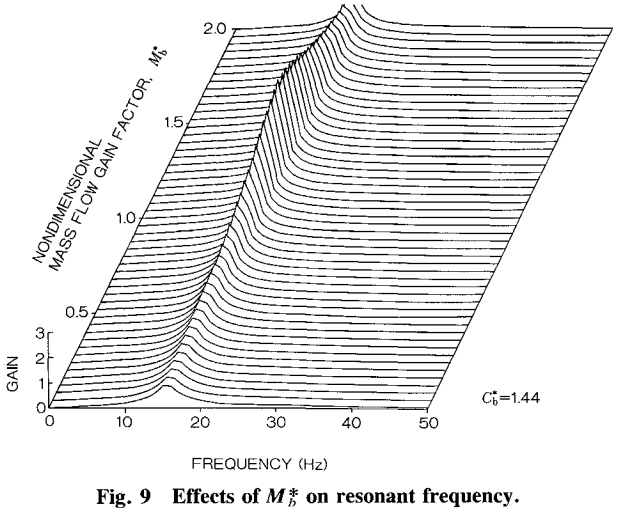

Fig. 9 Effects of M_b^* on resonant frequency.

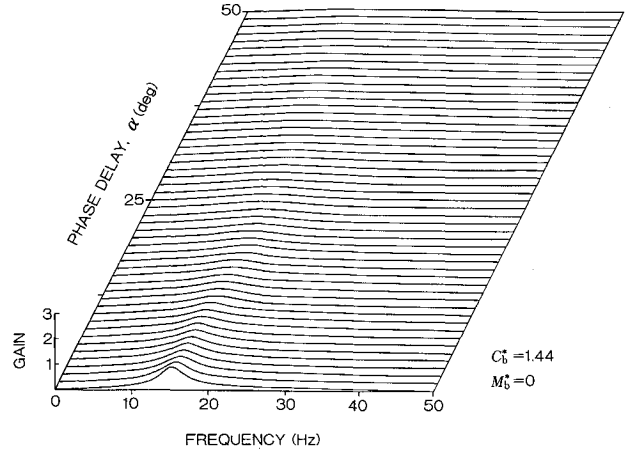

Fig. 10 Effects of phase delay on gain.

as a parameter, gains of $H_1(s)/H_2(s)$ were calculated. The M_b value that yielded the same gain as the experimentally obtained gain determined by FFT analysis of the pump inlet and outlet pressure data was assumed to be the actual M_b. As mentioned in the introduction, in the case of high frequency, phase delay of cavity volume change to pump inlet pressure fluctuation was not negligible. Figure 10 shows the effect of delay in degree on the transfer function gain between the pump inlet pressure fluctuation and the pump outlet pressure fluctuation. As shown in Fig. 10, the effect of phase delay on the gain is conspicuous, but resonant frequency is not affected by the delay. The values of α were derived from test results in the literature,[7] because they were the only data available. Figure 11 shows the α values.

In Eqs. (1–3), the connecting pipe system was treated as an incompressible lumped parameter system. More precisely, the connecting pipe system was treated as a compressible distributed parameter system in the next step. In this compressible treatment, downstream pressure fluctuation and flow

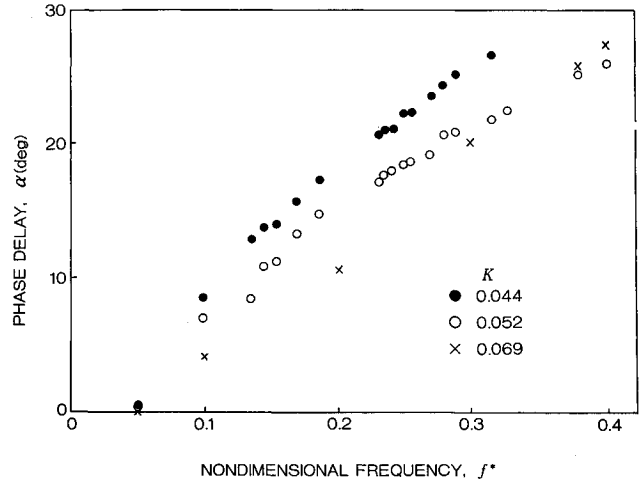

Fig. 11 Values of phase delay.

fluctuation values were determined using upstream values as follows[11]:

$$\tilde{h}_d = \tilde{h}_u \cosh \gamma l - \tilde{q}_u Z_c \sinh \gamma l \quad (9)$$

$$\tilde{q}_d = -(\tilde{h}_u/Z_c)\sinh \gamma l + \tilde{q}_u \cosh \gamma l \quad (10)$$

Results and Discussion

In Fig. 12, as an example of sweep test data, the transfer function between the pump inlet pressure and the pump outlet pressure obtained by FFT analyzer is shown. Without installing a large accumulator in the vicinity of the pump inlet, resonant frequency could not be clearly determined. However, by installing such an accumulator, it became easy to determine resonant frequency as shown in Fig. 12.

In Fig. 13, the LE-7 LOX pump cavitation compliance for two geometries of the inducer housing is presented. Dimensions of the two geometries are listed in Table 2. Cavitation compliance for the geometry in which rotor vibration due to rotating cavitation disappeared, case 2, was considerably larger than that for the geometry in which the rotor vibration occurred, case 1. This tendency is consistent with the results of the rotating cavitation analysis[4] shown in Fig. 2, in which the damping rate of disturbance increases with C_b.

Although water was used in the experiment, cavitation compliances and the mass flow gain factors of inducers were determined by measuring the dynamic flow rate.[7] Equations based on these experimental results that were used to estimate quasistatic C_b and M_b have been previously presented.[7] Calculated C_b values determined by substituting specific values of the LE-7 LOX pump into these equations are also shown in Fig. 13. These calculated C_b values agreed relatively well with the test results in the region of large cavitation numbers, but they were quite different in the region of small cavitation numbers. The difference of the pump fluids is assumed to be the reason for this. The latent heats of vaporization of LN_2 and LOX are much smaller than that of water (199.1 kJ/kg for LN_2, 213.1 kJ/kg for LOX, 2260 kJ/kg for water). The specific heats of LN_2 and LOX are also smaller than that of water (2.03 kJ/kg·K for LN_2 at 77.3 K, 1.70 kJ/kg·K for LOX at 90 K, 4.19 kJ/kg·K for water at 293 K). Therefore, generation of vapor bubbles due to heat inflow through walls and kinetic energy of backflow at the pump inlet is considered to be more active in the case of LN_2 and LOX. In the case of cryogenic fluid, as the pump inlet pressure decreases, cavitation is assumed to begin in places other than the pump. The fact that the ultrasonic flow meter installed in the pump inlet line didn't work in low inlet pressure tests, probably due to bubble generation, supports this assumption. On the other hand, the pump rotational speed was varied as a parameter, as shown in Table 3, to investigate whether a similarity law exists for rotational speed. Cavitation compliances of each rotational speed fell on a second-order regression curve well, as shown in Fig. 13, demonstrating the existence of a similarity law for rotational speed.

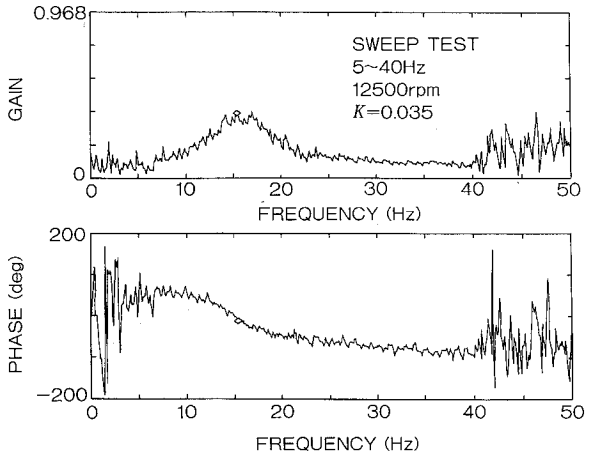

Fig. 12 Example of transfer function.

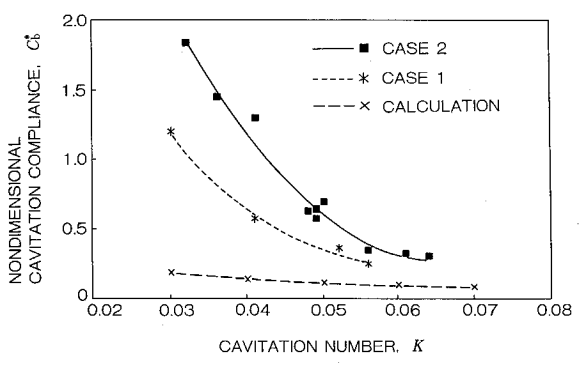

Fig. 13 Cavitation compliance.

In Fig. 14, the mass flow gain factor of the LE-7 LOX pump is shown for two geometries of the inducer housing compared with calculated values determined by substituting specific values of the LE-7 LOX pump into equations derived from water-test results. Calculated values and case 1 test values increase with cavitation number reduction. On the other hand, case 2 test values decrease with cavitation number reduction in the cavitation number region between 0.035–0.055. The reason why case 2 test values decrease with cavitation number reduction has not yet been clarified. However, the test results clearly explain why rotor vibration due to rotating cavitation was suppressed almost completely by modification of inducer housing. In Fig. 2, examples of test data of case 1 and case 2 are plotted for this explanation. Case 2 falls in the stable region, and case 1 falls in the unstable region. By modification of inducer housing of case 1, the value of C_b increased, and that of M_b decreased, and these values became the values for case 2. If the value of M_b remains constant or increases due to the modification, case 2 still remains in the unstable region, although the value of C_b increases due to the modification. Therefore, modification of the inducer housing resulted in a situation in which C_b became larger and M_b became smaller. Further research to clarify why M_b decreases with the reduction of K is necessary.

In Fig. 15, the LE-7 LOX pump cavitation compliances are compared with results reported in the literature.[12] In the past, cavitation compliances of F-1, J-2, H-1, LE-5 rocket engine LOX pumps were compared by nondimensionalization, dividing cavitation compliances by the pump inlet cross-sectional areas. The results did not show a good correlation among the pumps. However, in the present study, a fairly good correlation was obtained, as presented in Fig. 15, by nondimensionalization in which inducer tip speed and inducer geometry were taken into account. However, these nondimensionalized cavitation compliances are different from the

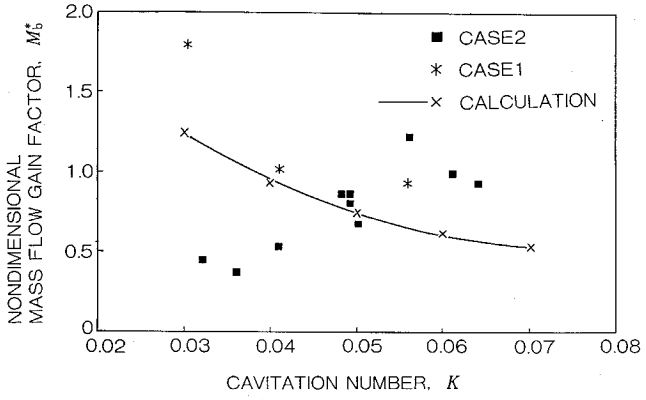

Fig. 14 Mass flow gain factor.

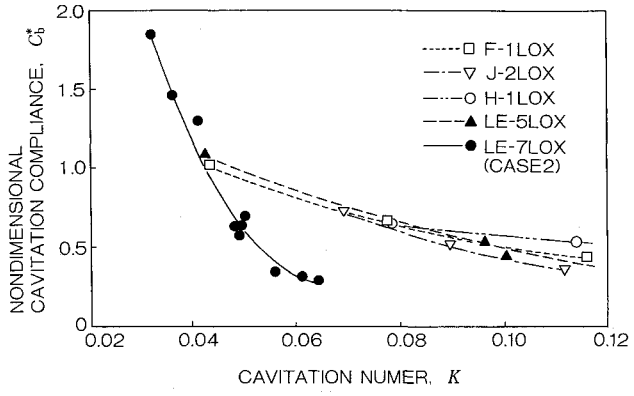

Fig. 15 Comparison of cavitation compliances of several LOX pumps.

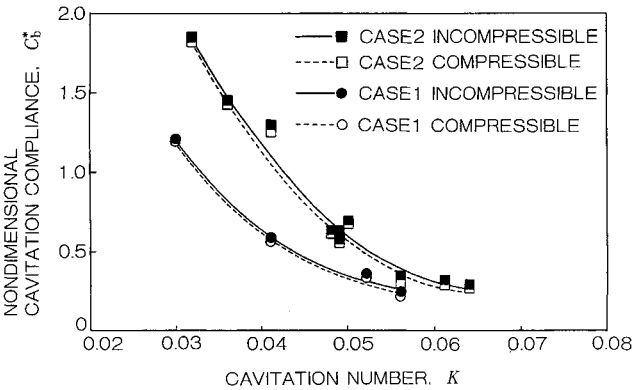

Fig. 16 Effects of pipe system compressibility.

values of the LE-7 LOX pump in the region of large cavitation numbers as shown in Fig. 15. This is considered to be the result of installing the large accumulator in the vicinity of the pump inlet in order to eliminate upstream compliances. The effect of the accumulator is considered to have become conspicuous in the region of large cavitation numbers where the ratio of the pump cavitation compliance to the total compliance was small. Such nondimensionalization did not result in a good correlation between the LOX pumps and the LH_2 pumps of the rocket engines, probably due to the great difference of the thermal and physical properties of the fluids.

In Fig. 16, effects of pipe system compressibility on the test results of C_b are shown. The solid lines show the results determined by the incompressible lumped parameter model, and the dashed lines show the results determined by the compressible distributed parameter model. The difference between the two results was small, especially in the small cavitation number region where resonant frequency was smaller.

Concluding Remarks

The effects of geometry on dynamic response of the cavitating LE-7 engine LOX pump were investigated by perturbation tests using cryogenic fluid. Determination of cavitation compliance and the mass flow gain factor by transfer function between the pump inlet pressure and the pump outlet pressure utilizing resonant frequency was attempted. Nondimensionalized test results were compared with the calculated values and values presented in the literature. Conclusions are summarized as follows:

1) Cavitation compliance for the geometry in which rotor vibration due to rotating cavitation disappeared was considerably larger than that for the geometry in which the rotor vibration occurred. This tendency is consistent with the results of the rotating cavitation analysis.

2) Calculated values and original inducer housing test values of the mass flow gain factor increased with cavitation number reduction. On the other hand, modified inducer housing test values decreased with cavitation number reduction in the cavitation number region between 0.035–0.055. These test results clearly explained why rotor vibration due to rotating cavitation was suppressed almost completely by modification of inducer housing.

3) The large accumulator installed in the vicinity of the pump inlet eliminated the upstream effects and made resonant frequencies clear.

4) In the region of small cavitation numbers, cavitation compliance values determined by cryogenic fluid tests were much larger than those determined in tests employing water.

5) Nondimensionalization of cavitation compliance, in which inducer tip speed and inducer geometry were taken into account, correlated with cavitation compliances of several rocket LOX pumps very well.

Acknowledgment

The author is deeply grateful for the helpful and valuable discussion of K. Kamijo, Deputy Director of National Aerospace Laboratory, Kakuda Research Center, Japan.

References

[1]Rubin, S., "Prevention of Coupled Structure-Propulsion Instability (POGO)," NASA SP-8055, Oct. 1970.

[2]Aoki, H., Yamada, Y., and Kamijo, K., "LE-7 Cryogenic Rocket Engine for H-II Launch Vehicle," International Astronautical Federation Paper 85-162, Oct. 1985.

[3]Kamijo, K., Yoshida, M., and Tsujimoto, Y., "Hydraulic and Mechanical Performance of LE-7 LOX Pump Inducer," *Journal of Propulsion and Power*, Vol. 9, No. 6, 1993, pp. 819–826.

[4]Tsujimoto, Y., Kamijo, K., and Yoshida, Y., "Theoretical Analysis of Rotating Cavitation in Rocket Pump Inducers," AIAA Paper 92-3209, July 1992.

[5]Shimura, T., and Kamijo, K., "Dynamic Response of the LE-5 Rocket Engine Liquid Oxygen Pump," *Journal of Spacecraft and Rockets*, Vol. 22, No. 2, 1985, pp. 195–200.

[6]Brennen, C. E., and Acosta, A. J., "The Dynamic Transfer Function for a Cavitating Inducer," *Journal of Fluids Engineering*, Vol. 98, June 1976, pp. 182–191.

[7]Brennen, C. E., Meissner, C., Lo, E. Y., and Hoffman, G. S., "Scale Effects in the Dynamic Transfer Function for Cavitating Inducers," *Journal of Fluids Engineering*, Vol. 104, Dec. 1982, pp. 428–433.

[8]Alais, P., and Demarais, J. C., "Measurement of Rapidly Varying Hydraulic Flow Rates by Ultrasonic Waves," NASA TTF-14392, Aug. 1972.

[9]Kamijo, K., Yoshida, M., and Nagao, T., "Performance Evaluation of LE-7 High-Pressure Pumps," *Journal of Propulsion and Power*, Vol. 10, No. 2, 1994, pp. 288–290.

[10]Brennen, C. E., "Bubbly Flow Model for the Dynamic Characteristics of Cavitating Pumps," *Journal of Fluid Mechanics*, Vol. 89, Pt. 2, 1978, pp. 223–240.

[11]Wylie, E. B., and Streeter, V. L., *Fluid Transients*, McGraw-Hill, New York, 1978, p. 210.

[12]Ghahremani, F. G., and Rubin, S., "Empirical Evaluation of Pump Inlet Compliance," NASA CR-123963, July 1972.